PROCEEDINGS OF SCIENCE

Particle identification in ALICE and LHCb

[1,2]Christian Sonnabend[*†]

[1]*CERN,* [2]*Ruprecht-Karls Universität, Heidelberg*

E-mail: christian.sonnabend@cern.ch

In these proceedings the status and methods used in Run 3 (2021-present) of LHC for particle identification in the ALICE and LHCb experiments are presented. Detector upgrades during long shutdown 2 (LS2, 2018-2021) as well as novel algorithms are discussed for several detection systems relevant for particle identification in both experiments.

Large Hadron Collider Physics
22nd-26th of May, 2023
Belgrade, Serbia

[*]Speaker
[†]On behalf of the ALICE and LHCb collaboration

PoS(LHCP2023)051

1. Introduction

The investigation of pp, p-Pb and Pb–Pb collisions using the large hadron collider (LHC) located at CERN in Geneva allows the study of nuclear and subnuclear matter. Several experiments, such as ALICE [1] and LHCb [2], located around the 27 km accelerator ring probe fundamental aspects of the best description of particle physics known to date, the standard model. In 2022, the LHC resumed its operation with an unprecedented instantaneous pp luminosity of up to $2 \times 10^{34} \mathrm{cm}^{-2}\mathrm{s}^{-1}$ and top energies of $\sqrt{s_{\mathrm{NN}}}$ = 13.6 TeV. The higher rates of up to 40 MHz in pp and 50 kHz in Pb–Pb collisions and resulting detector occupancies pose new challenges particularly in light of particle identification (PID). Several upgrades and developments in both experiments during long shutdown 2 (LS2, 2015-2018) were needed to cope with this challenging environment [3]. Relying on pure software triggering, both experiments face the task of maintaining their PID capabilities while drastically improving their computational algorithms. Major PID capabilities of ALICE are concentrated in the central barrel of the detector consisting of a time projection chamber (TPC), a transition radiation detector (TRD) and a time of flight detector (TOF), complemented by calorimeters at larger radii and muon detection in the forward rapidity region. Without the cylindrical arrangement of detectors around the interaction vertex, the LHCb experiment on the other hand focuses purely on the forward rapidity direction with two ring-imaging cherenkov detectors (RICH) followed by electromagnetic (ECal) and hadronic (HCal) calorimeters as well as four muon detection layers (M2-M5).

2. Particle identification in the LHCb experiment

In close proximity to the interaction vertex, LHCb employs a first stage of particle identification using RICH detectors [4]. Increasing the focal length of the mirror system of each RICH detector in combination with the exchange of hybrid photon detectors to multi-anode photomultipliers result in an average occupancy of $\leq$35%, even in regions close to the beam axis [5, 6]. The PID performance can therefore be maintained with similar quality as in Run 2. Particle identification is achieved by calculating a log-likelihood score for each mass hypothesis. Differences of log-likelihoods to the pion mass hypothesis are calculated and the PID minimizing this delta log-likelihood (DLL) is passed on to further downstream processing. Figure 2.1 shows the RICH performance of kaon and pion identification efficiency under different DLL cuts and luminosities . The luminosity settings were tested up to the maximum expected luminosity of 20×10^{32} $\mathrm{cm}^{-2}\mathrm{s}^{-1}$ at which data will be taken by LHCb in Run 3. A strongly increased performance for Lumi20 can be observed with the upgraded geometry with over 95% kaon identification efficiency at 10% pion misidentification rate. The upgraded geometry for Lumi20 shows a higher efficiency compared to the geometry used in Run 2 at Lumi10 settings. A secondary stage of RICH detectors at larger distances from the interaction vertex further increases the PID efficiency for high momentum particles.

Calorimeter information can further help to distinguish charged hadrons and leptons. A novel graph-based clustering algorithm has been deployed successfully by LHCb. It matches the performance of the previously used cellular automaton but decreases its computation time drastically for higher numbers of occupied ECAL cells [8].

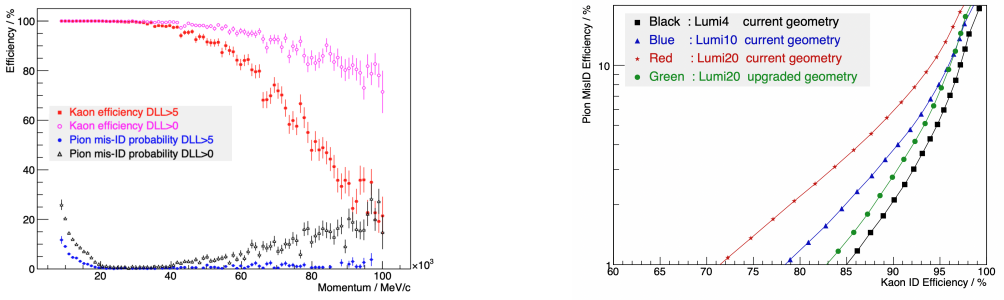

(a) **(b)**

Figure 2.1: Pion to kaon identification efficiency for different DLL cuts (a) and luminosity settings (b) of the upgraded RICH geometry. "LumiN" refers to N×10^{32} $cm^{-2}s^{-1}$ of instantaneous luminosity [7].

Identification of muons occurs at the detection layers furthest away from the primary interaction vertex. Readout and software of the muon detectors (M2-M5) have been upgraded for Run 3. In the HLT2 (High-Level Trigger) reconstruction, the χ^2_{corr} variable results in a better performance than the MuonDLL discriminator used in Run 2, matching its computational speed but additionally taking track and hit correlations as well as multiple scattering effects into account [9]. A boosted decision tree algorithm (CatBoost) further purifies the muon selection as can be seen in figure 2.2.

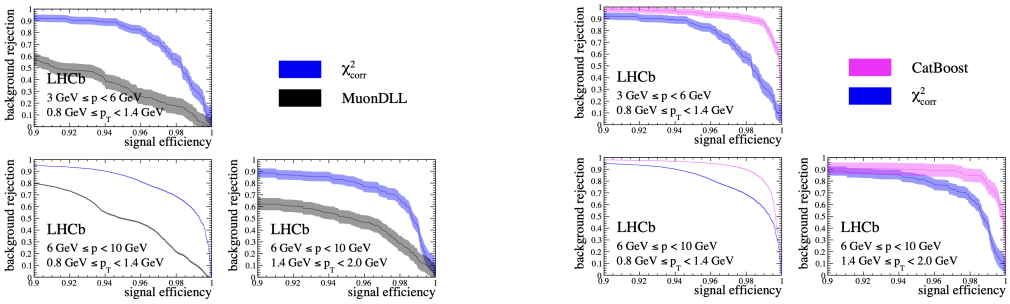

(a) **(b)**

Figure 2.2: Comparison of the MuonDLL, χ^2_{corr} (a) and CatBoost (b) selections on 2016 calibration data for proton rejection as a function of the muon efficiency.

3. Particle identification in the ALICE experiment

With new hardware upgrades for Run 3, the ALICE experiment is now reading out data in continuous mode. One of its major particle identification detectors, the time projection chamber (TPC) is the largest data producer of the experiment with up to 99.4% of the raw data stream in 50 kHz central Pb–Pb collisions [10]. Its superb PID capabilities make it an excellent detector for primary and secondary charged leptons, hadrons as well as light nuclei from pp, p–Pb and Pb–Pb collisions. In Run 3, gas electron multipliers (GEMs) replace the previously employed multi-wire proportional chambers which allow to record up to 50kHz interaction rate in central Pb–Pb collisions [11]. PID is performed via fits of the dE/dx signal as a function of momentum, described by a parameterization of the Bethe-Bloch formula.

Figure 3.1 shows the fitted Bethe-Bloch parametrizations from 524.3 billion collisions and a custom ^{3}He Bethe-Bloch fit. Additional secondary corrections for angular track dependencies, detector multiplicities and clusters-per-track dependencies are performed using neural networks, replacing the previously used spline approach. The fully data-driven, six-dimensional corrections are applied in the ALICE offline analyses for mean dE/dx and signal resolution corrections and shows superb performance for PID via Nσ cuts as can be seen in figure 3.2.

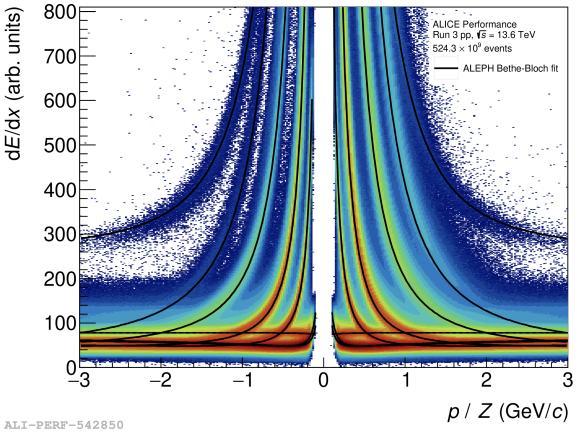

Figure 3.1: Fitted Bethe-Bloch parametrizations on the full ALICE 2022 data with 524.3 billion collisions.

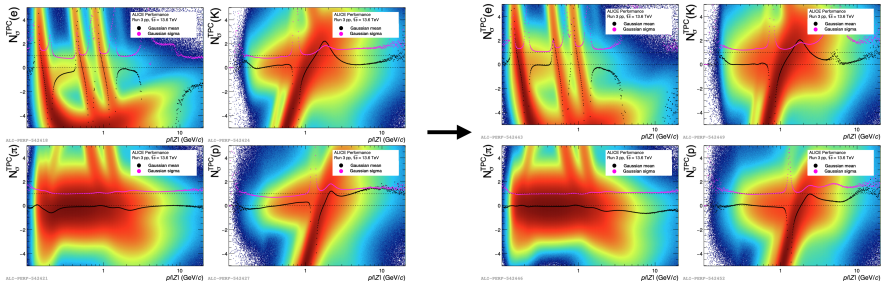

Figure 3.2: Nσ distributions of the ALICE TPC without (left) and with (right) the application of neural network corrections. A clear improvement in mean and resolution estimation for each species is demonstrated.

Following the TPC in radial direction at 3.7 m from the interaction point is the time-of-flight (TOF) detector. The performance of the TOF detector matches its expectations and performs comparable to Run 2. Moreover, ALICE employs a variety of other detectors such as a TRD, calorimeters, a RICH detector and muon detection in the forward rapidity region. Figure 3.3 demonstrates the resolution of the TOF spearation power as well as the η and π^0 invariant mass peaks in the $\pi^0 \rightarrow \gamma\gamma$ and $\eta \rightarrow \gamma\gamma$ decay channel, measured with the photon spectrometer (PHOS) and electromagnetic calorimeter (EMCal). Additionally, a new muon forward tracker (MFT), based on the CMOS technology of the inner tracking system (ITS) complements muon tracking and identification [12].

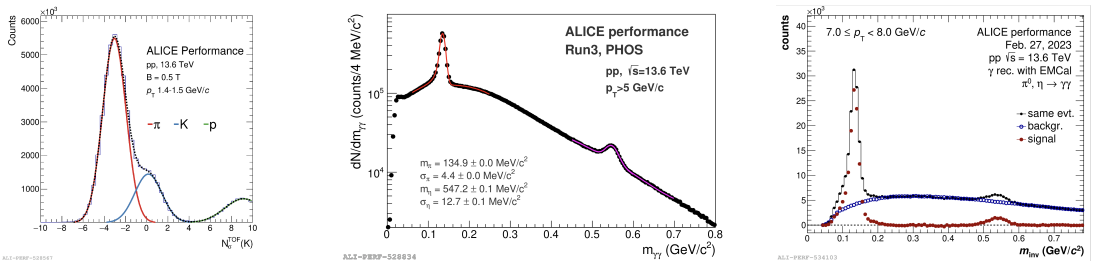

(a) **(b)** **(c)**

Figure 3.3: Performance of the TOF (a), PHOS (b) and EMCal (c) detectors at pp, $\sqrt{s}$ = 13.6 TeV data.

References

[1] K. Aamodt et al. The ALICE experiment at the CERN LHC. *JINST*, 3:S08002, 2008. doi: 10.1088/1748-0221/3/08/S08002.

[2] A. Augusto Alves, Jr. et al. The LHCb Detector at the LHC. *JINST*, 3:S08005, 2008. doi: 10.1088/1748-0221/3/08/S08005.

[3] Stephane Fartoukh, et al. LHC Configuration and Operational Scenario for Run 3. Technical report, CERN, Geneva, 2021. URL https://cds.cern.ch/record/2790409.

[4] R. Calabrese, et al. Performance of the LHCb RICH detectors during LHC Run 2. jul 2022. doi: 10.1088/1748-0221/17/07/P07013. URL https://dx.doi.org/10.1088/1748-0221/17/07/P07013.

[5] A Papanestis, F Keizer, and S A Wotton. The upgrade of the LHCb RICH system for the LHC Run 3. *JINST*, 15(09):C09022, 2020. doi: 10.1088/1748-0221/15/09/C09022. URL https://cds.cern.ch/record/2749008.

[6] LHCb Collaboration. LHCb PID Upgrade Technical Design Report. Technical report, 2013. URL https://cds.cern.ch/record/1624074.

[7] LHCb PID Upgrade Technical Design Report. 11 2013.

[8] Núria Valls Canudas, et al. Graph Clustering: a graph-based clustering algorithm for the electromagnetic calorimeter in LHCb. *Eur. Phys. J. C*, 83(2):179, 2023. doi: 10.1140/epjc/s10052-023-11332-1. URL https://cds.cern.ch/record/2846012. 12 pages, 9 figures, submitted to EPJ C.

[9] Lucio Anderlini, et al. Muon identification for LHCb Run 3. *JINST*, 15(12):T12005, 2020. doi: 10.1088/1748-0221/15/12/T12005. URL https://cds.cern.ch/record/2727496.

[10] David Rohr. Usage of GPUs in ALICE Online and Offline processing during LHC Run 3. *EPJ Web Conf.*, 251:04026, 2021. doi: 10.1051/epjconf/202125104026.

[11] J. Adolfsson, et al. The upgrade of the ALICE TPC with GEMs and continuous readout. *JINST*, 16(03):P03022, 2021. doi: 10.1088/1748-0221/16/03/P03022. URL https://cds.cern.ch/record/2758225. 88 pages, 60 figures.

[12] The ALICE collaboration. Technical Design Report for the Muon Forward Tracker. Technical report, 2015. URL https://cds.cern.ch/record/1981898.